ADVANCED ELECTRONIC MATERIALS
www.advelectronicmat.de

Role of Singlet and Triplet Excitons on the Electrical Stability of Polymer Light-Emitting Diodes

*Bas van der Zee, Sarina Paulus, Rui-Qi Png, Peter K. H. Ho, Lay-Lay Chua, Gert-Jan A. H. Wetzelaer, and Paul W. M. Blom**

Stability under electrical stress is an important aspect for the function of organic light-emitting diodes (OLEDs). Degradation is currently one of the key topics in this field, concerning all types of OLEDs, including fluorescent-, phosphorescent-, and thermally activated delayed fluorescence-based OLEDs. For single-layer polymer light-emitting diodes (PLEDs) it has recently been found that degradation is the result of hole trap formation due to exciton–polaron interactions. However, whether singlet or triplet excitons are responsible for degradation is an open question. Here, their contributions are disentangled by systematically manipulating the singlet and triplet exciton populations and their effect on PLED degradation is studied. To control singlet excitons the emission of a blue-emitting PLED is modified to green by adding a small amount of a perylene-monoimide based green-emitting dye. The triplet population is manipulated by blending the light-emitting polymer with a dye that has either a longer or shorter triplet lifetime as compared to the polymer host. The results reveal that the degradation in fluorescent PLEDs is governed by the interaction between polarons and triplet excitons.

1. Introduction

The interest in using conjugated polymers to make polymer light-emitting diodes (PLEDs) comes from versatile synthesis options and their ability to be fabricated into flexible large-area devices at a low cost.[1–3] A large disadvantage hindering commercialization of PLEDs is their low efficiency: external quantum efficiencies are typically limited to a few percent only. In contrast, small-molecule organic LEDs exploiting triplet excitons using phosphorescent molecules (ph-OLEDs) or thermally activated delayed fluorescence (TADF) clearly outperform fluorescent PLEDs in terms of efficiency. The low efficiency is also detrimental for the operational stability of PLEDs, since higher currents are required to reach a required light-output, which accelerates degradation. However, to reach high efficiencies, both ph-OLEDs and TADF based OLEDs generally have complex device architectures comprising different injection, transport, emission, and blocking layers. Despite dissimilar architectures, the multilayer TADF and phosphorescent OLEDs as well as single-layer PLEDs all show typical degradation features of a voltage increase and a luminance decrease under continuous electrical operation.[4] For multilayer OLEDs the physical processes behind degradation are hard to elucidate due to the presence of many materials and interfaces.[5,6] The standard PLED device structure, being an emitting polymer layer sandwiched between two different work function electrodes, is more basic, making degradation processes more straightforward to analyze.

In earlier work on degradation of poly(phenylene vinylene) (PPV) based LEDs the effects of molecular weight, molecular structure, and defects that arise during synthesis on lifetime have been discussed.[7] In particular halogen related defects in PPVs are pointed out to have a negative influence on the lifetime. With regard to physical degradation mechanisms, in 2001, Silvestre et al.[4] were the first to propose that "voltage increase" and "luminance decrease" during degradation shared a common origin, namely the formation of trap states. Furthermore, Pekkola et al.[8] studied the influence of triplet excitons on the electrical stability of conjugated polymers. A triplet sensitizer was introduced into a PPV-based LED and a negative influence of triplet excitons on the lifetime was reported. As a possible mechanism the energy transfer from a PPV triplet to an oxygen triplet state, creating the reactive singlet oxygen molecule, was suggested.[9,10] Singlet oxygen has the ability to attack the vinyl bonds of PPVs, providing a chemical pathway for degrading the material.[11] Degradation due to extrinsic effects, such as oxygen and water, is typically minimized by proper encapsulation of organic LEDs and by working in a controlled environment.[5–7,12] Also in ph-OLEDs the harmful influence of

B. van der Zee, S. Paulus, Dr. G.-J. A. H. Wetzelaer, Prof. P. W. M. Blom
Max Planck Institute for Polymer Research
Ackermannweg 10, Mainz 55128, Germany
E-mail: blom@mpip-mainz.mpg.de
Dr. R.-Q. Png, Prof. P. K. H. Ho, Prof. L.-L. Chua
Department of Physics
National University of Singapore
Lower Kent Ridge Road, Singapore S117550, Singapore
Prof. L.-L. Chua
Department of Chemistry
National University of Singapore
Lower Kent Ridge Road, Singapore S117552, Singapore
The ORCID identification number(s) for the author(s) of this article can be found under https://doi.org/10.1002/aelm.202000367.

DOI: 10.1002/aelm.202000367

triplet excitons on lifetime has been extensively reported.[13–16] The device lifetime of ph-OLEDs has been increased by the incorporation of a managing molecule that dissipates the energy of highly excited states, resulting from triplet–triplet or triplet–polaron interactions, before they can lead to bond dissociation.[17] Furthermore, in TADF based OLEDs, triplet excitons have been pointed at as a cause of device degradation as well.[18]

In recent years, device models for single-layer PLEDs have been developed that quantitatively describe the electrical and light-output characteristics of PLEDs before degradation.[19] The availability of a well-established numerical drift-diffusion model[20] has recently been used to quantitatively address the degradation of PLEDs. Both the current density (*J*) and normalized current efficiency of degraded PLEDs were described by taking into account the formation of hole traps.[21] Furthermore, from the voltage increase with stress time the dynamics of hole trap formation, characterized by an initial linear increase with time followed by a square-root dependence, could be identified.[22] The hole trap formation also linked the voltage increase during stress with the decrease of the light-output due to additional nonradiative losses of free electrons with trapped holes. The linear and subsequent square-root dependence of the hole trap formation with stress time is consistent with exciton–polaron interactions as main mechanism for degradation.[22] In contrast to the earlier oxygen- and halogen-related degradation, this mechanism is of intrinsic nature. Although for the first time PLED degradation has been quantitatively described, a major mechanistic question remains, namely whether singlet, triplet, or both excitons are playing the major role in hole trap formation and the resulting PLED degradation. In this work we experimentally show, with the support of numerical modelling, that triplet excitons rather than singlet excitons are responsible for the intrinsic degradation of PLEDs. Knowledge of the exact degradation mechanism is indispensable for further improvement of the lifetime of organic LEDs. Due to their simplified device structure, PLEDs are an excellent model system to further study the fundamental processes behind degradation, providing a basis for optimization of the lifetime of highly efficient TADF single-layer OLEDs[23] and multilayer ph-OLEDs.

In order to disentangle the effect of singlet and triplet excitons in PLEDs on degradation we have to manipulate their properties such as energy and lifetime. This can be achieved by blending the light-emitting polymer with suited functional molecules.

Manipulation of the singlet energy is straightforward, as schematically shown in **Figure 1**c. The blue electroluminescence (EL) of PLEDs based on poly(dioctylfluorene)[24–28] (PFO, Figure 1a) can be easily converted to green by blending PFO with a low concentration of green emitting dye, in our case the perylene-monoimide (PMI) derivative DiPP-PMI (Figure 1b).[29] Perylene dyes have proven to be suitable candidates for tuning the emission color of PFO over a wide spectral range.[30] Since the blue emission spectrum of PFO overlaps well with the absorption of DiPP-PMI the Förster resonance energy transfer for singlet excitons is very efficient. As a result, a dye concentration of only 0.1% is sufficient to fully convert the blue PFO emission to green (Figure S1a, Supporting Information). In case that singlet excitons play a role in PLED degradation lowering their energy would be beneficial for the device stability, since

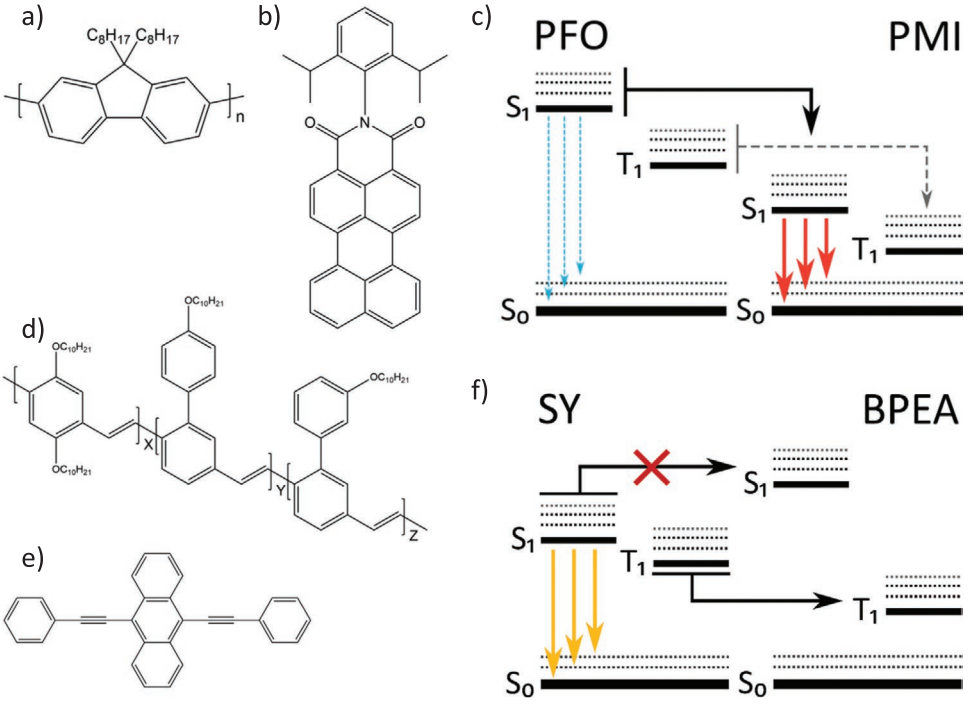

Figure 1. a,b,d,e) Structures of respectively PFO, DiPP-PMI, SY, and BPEA. c) Schematic illustration of the PFO:PMI system. S_0, S_1, and T_1 are the singlet ground state, first singlet excited state, and first triplet excited state, respectively. The weakened fluorescence of PFO and the weak triplet transfer are shown as dashed lines, whereas the prominent singlet transfer and stronger fluorescence of PMI are shown as bold lines. f) Schematic illustration of the SY:BPEA system. Singlet transfer of SY to BPEA is energetically not favored and therefore marked with a red cross.

excited states resulting from exciton–polaron or exciton–exciton interactions would be lower in energy, reducing the probability of breaking chemical bonds. It should also be noted that the steady-state concentration of singlet excitons in a PLED under DC current stress is not significantly changed by the incorporation of the DiPP-PMI dyes, since the (singlet) exciton lifetime of both PFO and DiPP-PMI are in the nanosecond regime. One could argue that also triplet excitons generated on the PFO can be transferred toward the triple state of the DiPP-PMI. However, singlet transfer is known to take place over a larger distance than triplet transfer, since triplets are transferred via a Dexter mechanism. For β-phase PFO, a Förster radius of 8.2 nm has been reported,[31] while Dexter transfer only occurs over a distance of 1–2 nm. In one of the very first papers utilizing phosphorescence in OLEDs[32] it was already shown that for 1% concentration of a phosphorescent dye in a host still EL of the host was visible, showing that Dexter transfer from host to dye was not complete. Only at 6% dye concentration the host emission disappeared and the emission solely originated from the phosphorescent dye. For this reason, almost all phosphorescent OLEDs utilize phosphorescent dye concentrations in the range of 6–10% in order to have complete Dexter energy transfer. At a dye concentration of only 0.1%, as used here, Dexter energy transfer is far from complete, as indicated by the dotted line in Figure 1c. The effect of the PMI dye incorporation is therefore mainly a reduction of the singlet exciton energy.

The effect of triplet excitons on degradation is harder to investigate in fluorescent OLEDs because of their nonradiative nature. For this purpose, we blend super-yellow poly(*p*-phenylene vinylene)[33] (SY-PPV, Figure 1d) with the anthracene derivative 9,10-bis(phenylethynyl)anthracene (BPEA, Figure 1e).[34] As schematically shown in Figure 1f, we make use of the fact that the anthracene derivative has a higher singlet-triplet splitting than the SY-PPV. On the one hand, as a result of the higher lying T_1 level of SY (1.3 eV)[35] with respect to that of BPEA (1.11 eV),[36] triplets can be efficiently transferred from the SY-PPV to the BPEA. On the other hand, since the singlet level of SY-PPV (2.21 eV)[35] lies below that of the BPEA (2.4 eV)[36] there will not be any Förster transfer of singlet excitons from SY-PPV to BPEA. Another substantial advantage of this system is that due to the higher bandgap of BPEA as compared to SY-PPV, the BPEA molecules will not act as charge traps. Therefore, BPEA can be added in concentrations of 5–10%, sufficient to capture all triplet excitons from SY-PPV, without disrupting the charge transport. Furthermore, since the highest occupied molecular orbital (HOMO) and lowest unoccupied molecular orbital (LUMO) levels of the BPEA dye are coinciding with those of the SY-PPV host, the charge transport and recombination will be dominated by the host, even at 15% BPEA concentration. Dye concentration dependent processes as guest–guest transport, which is often used in conventional OLEDs to balance transport, do not play a role in these SY-PPV:BPEA blends. Collecting all triplet excitons on the anthracene derivative has large consequences for the steady-state amount of triplet excitons during current stress. Triplet lifetimes of SY-PPV are on the order of 100 μs, whereas BPEA molecules have reported triplet lifetimes of 2.7–2.8 ms.[34] A more than ten times enhancement of the triplet lifetime will then lead to a corresponding increase of the steady-state triplet population under electrical stress. Since the singlet exciton properties are not affected, addition of BPEA allows us to independently manipulate the triplet concentration, which will affect triplet–polaron and triplet–triplet interactions.

2. Results and Discussion

2.1. PLED Degradation with Reduced Singlet Energy

Previous reports on the degradation of PLEDs using PFO and its derivatives[37,38] as emitter apply poly(3,4-ethylenedioxythiophene): polystyrene sulfonate (PEDOT:PSS) as anode, despite the misalignment in HOMO levels of PEDOT:PSS (–5.0 eV) and PFO (–5.8 eV). From earlier studies it is known that the initially limited hole injection from PEDOT:PSS into PFO is strongly enhanced once injected electrons from the cathode side reach the PEDOT:PSS and get trapped at the PFO/PEDOT:PSS interface.[39] This "forming" of the hole injection contact shows up as strong hysteresis in the first current–voltage (*J*–*V*) scan. During subsequent *J*–*V* scans the enhanced hole injection remains. The presence of this forming process complicates the degradation analysis of PEDOT:PSS/PFO based PLEDs, since during prolonged electrical driving it is unclear what happens to the PEDOT:PSS/PFO interface and the resulting hole injection. For this purpose, for devices using PFO and PFO:PMI blend as emitting layers, we replace PEDOT:PSS by triarylamine-fluorene copolymer poly(9,9-bis(3-(pentafluoroethanesulfonyl-imidosulfonyl) propyl)fluorene-2,7-diylalt-1,4-phenylene-(*p*-trifluoromethyl-phenylimino)-1,4-phenylene) sodium salt (pTFF-C2F5SIS).[40] The complete device structure can be found in Figure 7a of the Experimental Section. Since pTFF-C2F5SIS with a work function of ≈5.85 eV[40] does not require a forming process to obtain efficient hole injection into PFO, this allows us to more reliably analyze our degradation results.

As first step, to show that the energy transfer from PFO to DiPP-PMI takes place, the EL spectra of pristine PFO and PFO doped with 0.1–0.2% wt% of DiPP-PMI are presented in Figure S1a in the Supporting Information. While the PFO emission peaks are still present in a minimal way, the by far dominant contribution to the EL spectrum stems from the PMI. Furthermore, the *J*–*V* and normalized light-output versus voltage (*L*–*V*) characteristics of PFO and PFO:DiPP-PMI (0.2 wt%) PLEDs, as shown in Figure S2a,b in the Supporting Information, show that incorporation of such a small amount of dye does not strongly affect the charge transport and light generation in the respective PLEDs. This is expected since due to severe electron trapping the current in a pristine PFO based PLED is carried by holes.[41] As shown in Figure S2c in the Supporting Information the DiPP-PMI dye mostly affects the electron transport of the PFO.

Figure 2 shows the degradation characteristics of the PFO:DiPP-PMI devices aged at a constant current density of 10 mA cm^{-2}. Over the electrical driving period of around 6 h, the samples with and without DiPP-PMI show nearly the same voltage increase (Figure 2a) of around 5 V as well as an identical decrease of the light-output. (Figure 2b). By changing the emission color from blue to green we have altered the energy of the singlet excitons by 0.44 eV. The absence of any stability difference suggests that the energy of singlet excitons has no significant influence on the degradation characteristics of PLEDs.

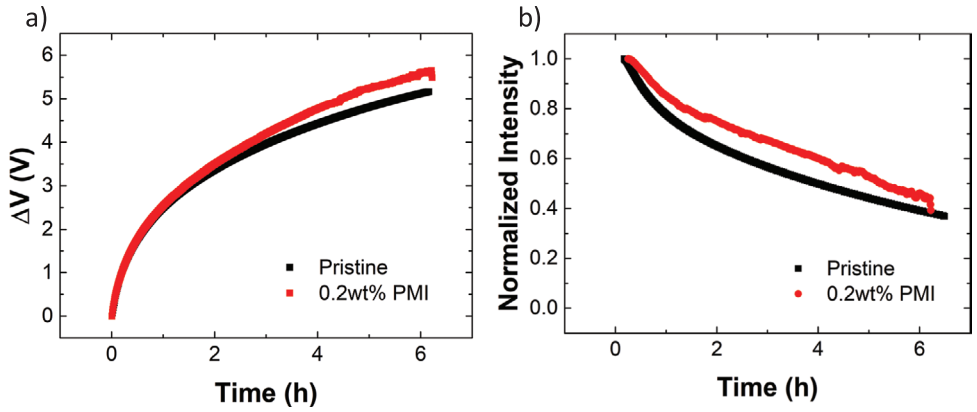

Figure 2. Degradation characteristics of pristine PFO and PFO with 0.2 wt% DiPP-PMI under constant current stress with a) Increase of the driving voltage and b) normalized light output as a function of stress time. The PLEDs were aged at a current density of 10 mA cm^{-2}.

To verify that we do not influence the analysis of the degradation characteristics of the PFO PLED by addition of a molecule with an electron trapping character, we have performed numerical simulations. The numerical PLED device model[22] is based on drift-diffusion equations that take the voltage, $V(t)$, from the degradation experiment as input and calculate the hole trap density (P_t) needed to keep the current constant at the aging current at each point in time. The light output as a function of stress time can then numerically be calculated by considering the radiative Langevin recombination together with the nonradiative trap-assisted recombination, that arises from the already existing electron traps and the newly formed hole traps. First, we calculate the amount of hole traps as function of time formed during current stress for a PLED with the typical parameters for PFO.[41] To incorporate the effect of the additional DiPP-PMI molecules, we then increase the amount of electron traps by a factor of two and perform the same analysis. The effect on the derived hole trap density as function of stress time (Figure S2d, Supporting Information) is only marginal, showing that the electron trapping feature of the PMI does not affect the degradation analysis.

2.2. PLED Degradation with Enhanced Triplet Lifetime

Next, we perform degradation experiments with SY:BPEA PLEDs to study the effect of an enhanced triplet lifetime, resulting in an enhanced triplet steady-state concentration. To capture most of the triplet excitons generated in SY-PPV during PLED operation we vary the BPEA concentration from 5 to 15 wt%. The resulting SY:BPEA PLEDs have a device structure as presented in Figure 7b of the Experimental Section. The EL spectra of SY blended in different weight percentages with BPEA (Figure S1b, Supporting Information) show no variation of the singlet peak of SY (λ = 550 nm), confirming the absence of singlet transfer from SY to BPEA molecules. The reported HOMO level of BPEA (–5.49 eV)[42] is slightly deeper than the HOMO of SY (≈–5.4 eV) and the LUMO of BPEA (–2.92 eV)[42] is marginally shallower to the LUMO of SY (≈–2.8 eV). Significant charge trapping is therefore not expected, also not for high BPEA concentrations. This is confirmed by the J–V and L–V of the SY:BPEA LEDs, presented in Figure S3a,b in the Supporting Information. From the J–V curves we see that increasing the BPEA concertation from 5 to 15 wt% indeed has no effect on the charge transport and light-output of the PLED.

The degradation characteristics of the SY:BPEA PLEDs are presented in **Figure 3** and were studied under a constant current density of 10 mA cm^{-2}. Figure 3a,b shows that the voltage increase and luminance decrease over time become significantly stronger with an increasing weight percentage of BPEA, until 10 wt%, at which point they saturate. The time when the light intensity reaches 80% of its initial intensity, LT80, decreases roughly by a factor of 8, 15, and 18 when adding 5, 10, and 15 wt% BPEA, respectively. Using numerical simulations we extract the hole trap density (P_t) as a function of time, which is plotted in Figure 3c. The simulations were based on the description as outlined above. The resulting light-output from the simulation can be compared with the luminance decrease over time from the degradation experiment, which are plotted together in Figure 3b and show good agreement.

After adding more than 10 wt% of BPEA, we can see from Figure 3a,b that the degradation characteristics do not change anymore. This is also reflected in the P_t versus t plot as well as in the plot of P_t versus BPEA concentration at a specific point in time (Figure 3c,d). Phosphorescent OLEDs typically employ an emitter concentration of around 6–10 wt% in order to harvest all triplets that are created on the host. It is therefore unsurprising that 10 wt% of BPEA is sufficient to collect all triplets in the SY-PPV PLED, which accounts for the saturation of the degradation characteristics for BPEA concentrations higher than 10 wt%. Summarizing, we observe that lowering of the energy of *singlet* excitons does not influence PLED degradation, whereas enhancement of the *triplet* lifetime strongly accelerates the degradation process. This indicates that triplet excitons play an important role in the PLED degradation. We note that by addition of BPEA we also slightly lower the energy of the triplet excitons. It is well known that the triplet energy plays an important role in the stability of phosphorescent OLEDs, red emissive OLEDs are more stable than blue due to a ≈1 eV lower triplet energy. However, in our SY-PPV:BPEA blends the lowering of the triplet energy is relatively small (<0.2 eV). Our experiments show that the effect of this slightly lowered triplet energy, which would be beneficial for stability, is overruled by the longer triplet lifetime, which strongly decreases stability, as experimentally

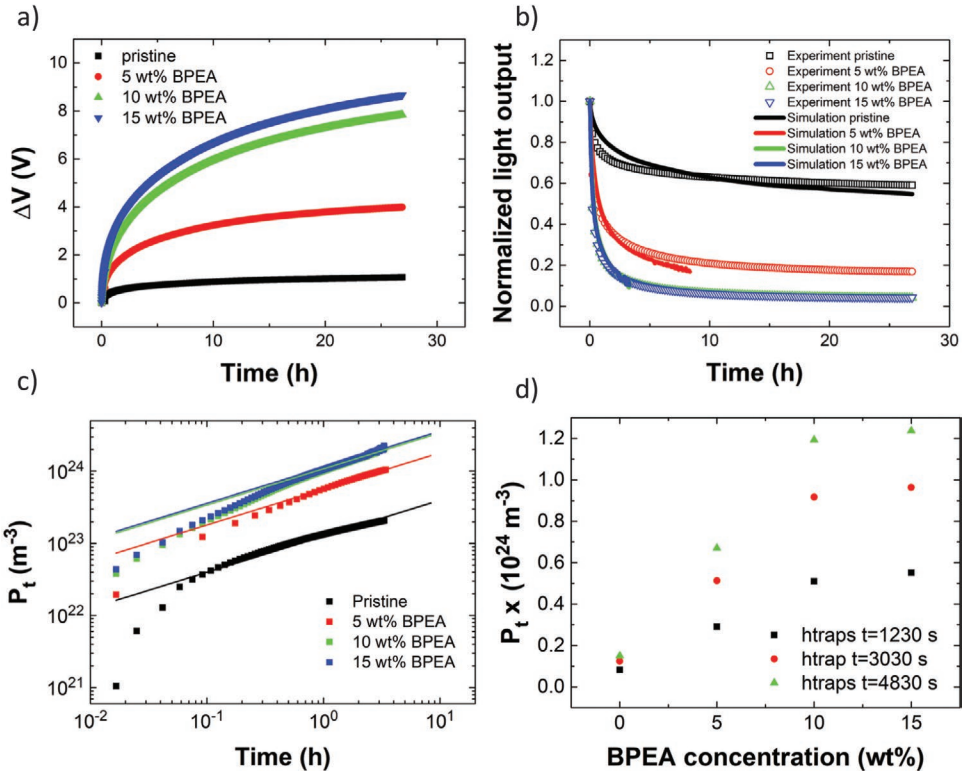

Figure 3. Degradation characteristics of SY PLEDs with different weight percentages of BPEA. a) Increase of driving voltage and b) normalized light output as a function of stress time for 0–15 wt% BPEA mixed into the SY-PPV active layer. c) Hole trap density as a function of time obtained from numerical simulation. The solid and lines have slope 0.5 and are a guide to the eye. d) Hole trap density at various stress times plotted as a function of BPEA concentration.

observed. A next question is then if the PLED stability can also be enhanced by a reduction of the triplet lifetime.

2.3. Increase of PLED Stability

In order to reduce the triplet lifetime in a blue-emitting PFO based PLED we blend PFO with the red emitting molecule 2,6-bis[4-(diphenylamino)phenyl]-9,10-anthracenedione $AQ(PhDPA)_2$[43,44] (chemical structure in **Figure 4**b). $AQ(PhDPA)_2$ shows next to prompt fluorescence also TADF as a result of reverse intersystem crossing due to the reduced energy splitting between the singlet and triplet levels. In this way the population of its triplets is depleted via the singlet state and their lifetime is shortened, leading to a reduction of the steady-state triplet population in the PLED under stress. The corresponding device structure is given in Figure 7a. The PFO:$AQ(PhDPA)_2$ blend, shown in Figure 4a, is from an energy level perspective similar to the PFO:PMI blend (Figure 1c). Equal to the PFO:PMI blend transfer of singlet excitons from PFO to $AQ(PhDPA)_2$ will be efficient due to the long range Förster process. As a result, shown in Figure S1c in the Supporting Information, only a low concentration of a few tenths of weight percent of dyes is required to shift the emission color from blue to red. To harvest all triplets on the dye a higher concentration would be required. We note that here increasing the concentration of the TADF dye to harvest more triplets is not straightforward. From the position of the HOMO and LUMO levels we expect the TADF dye to function as a deep electron trap, since the LUMO of $AQ(PhDPA)_2$ (–3.6 eV)[44] is much deeper than the LUMO of PFO (–2.6 eV). In contrast, their HOMO levels (–5.8 eV for PFO and –5.9 eV[44] for $AQ(PhDPA)_2$) are well aligned, so addition of the TADF dye will not impede hole transport. The *J*–*V* curves in Figure S4a in the Supporting Information show that, as expected, the increased electron trapping due to the red TADF has only a minor effect on the hole dominated current in the PFO LED. However, addition of a large amount (5–10 wt%) of deep electron traps will confine the electroluminescence in a very narrow region close to the cathode, where most of the excitons will be quenched by the metallic electrode. This will obscure the degradation processes. For this reason we have focused on PLEDs with 0.5 wt% of $AQ(PhDPA)_2$, where next to the *J*–*V* also the *L*–*V* characteristics are not strongly affected yet by incorporation of the dyes. A disadvantage is then that we will collect only a fraction of the in PFO generated triplets on the dye (Figure 4a, gray dashed line), but on the other hand still partially reduce the triplet population in the PLED.

To investigate the influence of the TADF dye on the PLED driving voltage and light output during degradation, we again perform the degradation tests at a constant current density of 10 mA cm^{-2}. The degradation characteristics of the PFO:$AQ(PhDPA)_2$ LEDs are presented in **Figure 5**. We observe that the voltage increase is reduced with increasing amount of

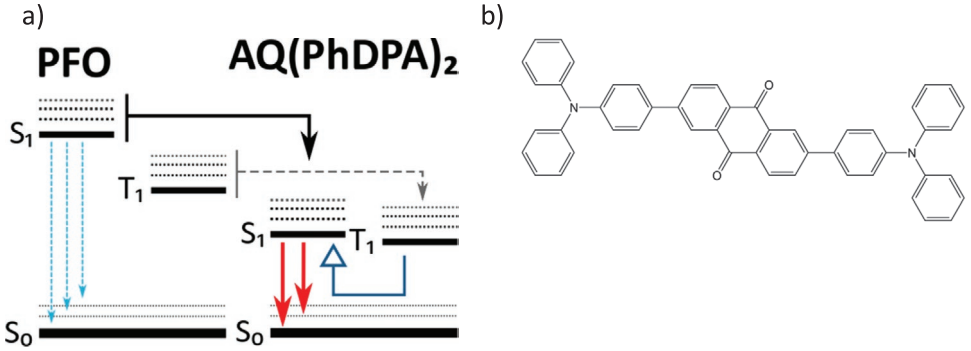

Figure 4. a) Schematic energy level diagram for the PFO:AQ(PhDPA)$_2$ blend. The weak emission of PFO and the reduced triplet transfer from PFO to the TADF molecule are shown as dashed lines, whereas the stronger fluorescence of the TADF dye and the singlet transfer of PFO to the TADF molecule are shown as bold lines. The reverse intersystem crossing is shown as a blue arrow with an open arrowhead. b) Chemical structure of AQ(PhDPA)$_2$.

TADF dye in the active layer and the light is more stable, demonstrating that a reduced triplet lifetime enhances stability.

3. Discussion

Typically, in a fluorescent PLED 25% of the excitons formed by Langevin recombination exhibit the singlet spin state, whereas 75% are formed with the triplet spin state. The fraction of singlet excitons in SY-PPV has been reported to be enhanced up to 40% by triplet-triplet annihilation (TTA).[45] Recombination of singlet excitons is fast: time-resolved photoluminescence measurement revealed a singlet exciton lifetime τ_S of 1.9 ns for SY-PPV at room temperature.[46] In contrast, the transition of the triplet state to the ground state is spin-forbidden and therefore a slow process compared to the singlet fluorescence. The triplet exciton lifetime τ_T in PPV derivatives was previously reported to be around 100 µs.[47] This substantial difference in exciton lifetime strongly affects the steady-state concentration of singlet [S] and triplet [T] excitons in a PLED under operation, with bimolecular recombination rate L given in first order by $[S] = 0.25L\tau_S$ and $[T] = 0.75L\tau_T$. As a consequence, the steady-state amount of triplet excitons in an operating PLED can be 4–5 orders of magnitude larger than the amount of singlet excitons. Furthermore, in an unaged operating PLED, the density of free electrons is much smaller than the density of free holes due to the present of electron traps.[48] Therefore, the interactions between triplet excitons (triplet–triplet annihilation) and between triplet excitons and free holes (triplet–polaron interaction) are expected to be dominant processes in an operating PLED.

Having now the experimental confirmation that indeed triplet excitons are involved in the degradation of fluorescent PLEDs, the question arises if the mechanism of hole trap formation proceeds via the triplet–polaron interaction.[22] Other mechanisms involving triplets that possibly play a role in the degradation are TTA or monomolecular triplet recombination. TTA in OLEDs has been intensively studied in the last decade.[49] Due to the relatively low stability of phosphorescent blue OLEDs in present applications such as displays, blue light is often generated by fluorescence. It has been demonstrated that in fluorescent OLEDs the efficiency can be enhanced by up to 20–30%[49] or even up to 60%[50] by TTA, where two nonradiative triplets fuse to a radiative singlet exciton. Specifically for blue-emitting devices recent progress in both efficiency and stability has been achieved by employing TTA.[51,52] Regarding stability of OLEDs and PLEDs TTA can also play an important role. First, a higher efficiency due to TTA means for a given light-output a lower current, so less polarons, which reduces triplet–polaron interactions. Furthermore, TTA also lowers

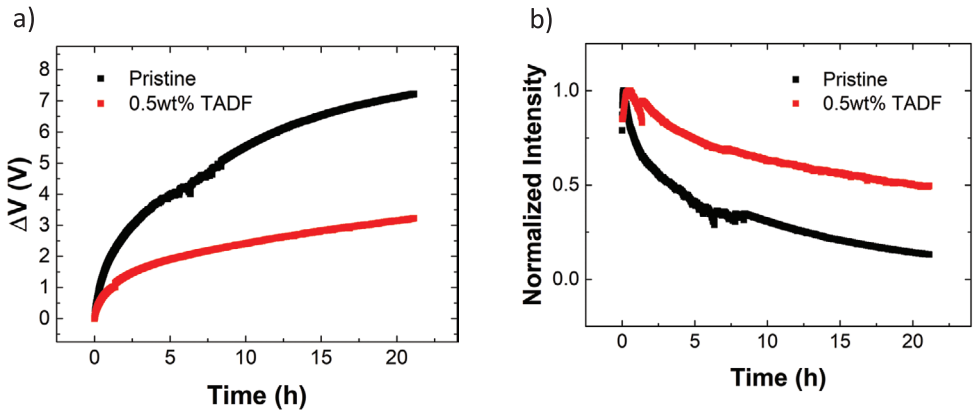

Figure 5. a) Voltage increase and b) normalized light output versus time of the PFO:AQ(PhDPA)$_2$ LEDs for different wt% of TADF aged at a constant current density of 10 mA cm^{-2}.

the triplet lifetime, resulting in a lower steady-state triplet concentration in an OLED driven at constant current, which will enhance the stability as well.[14] Also in our SY:BPEA blend TTA could in principle enhance the efficiency of the PLED; a high triplet concentration on BPEA might enhance TTA upconversion to the singlet S1 state of BPEA, which then could be transferred to the S1 state of SY. If this recombination mechanism would be important a significant enhancement of the PLED efficiency upon addition of BPEA would be expected. However, experimentally this is not observed, showing that the contribution of such a recombination channel is either small or absent. This recombination pathway is also expected to be unimportant, since the efficiency of the upconversion reaction via TTA was reported to be only 1.6% for BPEA.[53] However, the important question remains how the contributions of the various triplet-related degradation mechanisms can be disentangled.

Experimentally, it was found that the hole trap formation scales linearly with the current density (J) and scales with stress time (t) as $t^{1/2}$ presented in Equation (1)

$$P_t = \alpha \times J \times t^{1/2} \tag{1}$$

with α a proportionality constant. This trap formation rate could be rationalized by Niu et al.[22] as being the result of (triplet) exciton–polaron interactions.

Following the same approach the dynamics of hole trap formation for the case of a monomolecular process (presented in Section S5-1, Supporting Information) can also be derived, given by

$$P_t = \gamma \times J^{3/4} \times t^{1/2} \tag{2}$$

with γ another proportionality constant. Furthermore, for the case of triplet–triplet interaction, we obtain an expression for the hole trap density formation (Section S5-2, Supporting Information) following

$$P_t = \beta \times J \times t^{1/3} \tag{3}$$

with β again a proportionality constant. This demonstrates that we can distinguish between these three mechanisms by analyzing the aging current and time dependence of the hole trap density. For SY-PPV it has already been reported that the hole trap density shows a linear dependence on aging current, combined with a square-root dependence on stress time.[22] Combination of these observations then exclude triplet–triplet interactions and monomolecular decay processes as cause of the hole trap formation during stress. Another argument can be made based on the scaling of the hole trap density with BPEA concentration. Figure 4d shows that the amount of generated hole traps scales linearly with the concentration of BPEA for the time points considered. Intuitively, a quadratic dependence is expected if TTA would be the most pronounced mechanism behind degradation. A linear concentration dependence instead argues in favor of the triplet–polaron interaction. Furthermore, the observed linear dependence of hole trap formation on BPEA concentration also indicates that the BPEA triplet lifetime remains unaffected. A strong decrease of the triplet lifetime with increasing BPEA concentration would result in a sublinear behavior.

Another question is whether the observed dependence of hole tap formation on stress time and stress current also holds for other PPV derivatives. For this purpose we used the polymer poly[2-methoxy-5-(2′-ethyl-hexyloxy)-1,4-phenylenevinylene] (MEH-PPV) as the emitting material. MEH-PPV has a higher mobility[19] of 5×10^{-11} m^2 V^{-1} s^{-1} as compared to SY-PPV,[21] which amounts to 5×10^{-12} m^2 V^{-1} s^{-1}. **Figure 6** shows the hole trap density over time for a range of aging currents scaled with either a linear J (Figure 6a) or a $J^{3/4}$ (Figure 6b) current dependence. We vary the aging currents from 25 to 100 mA cm^{-2} and show the modeled hole trap densities after the initial "burn-in".[22] The scaling is done as follows: P_t at an aging current of 100 mA cm^{-2} is taken as a reference and the hole trap densities in the range of 25–75 mA cm^{-2} are multiplied by a factor $100/J_{age}^{x}$, where J_{age} is the aging current in mA cm^{-2} and "x" is either 1 or ¾ for a J- or a $J^{3/4}$-scaling, respectively. In other words, the hole trap densities in the range of 25–75 mA cm^{-2} are corrected as if they had an aging current of 100 mA cm^{-2}. It appears that the hole trap concentration curves scaled linearly with the aging current lie almost on top of each other, while the $J^{3/4}$-scaled curves are further apart. Based on these results we can already exclude the monomolecular process.

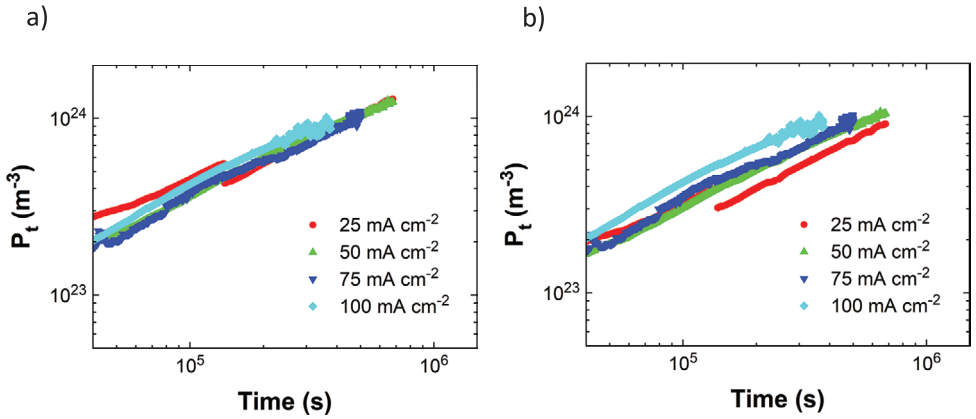

Figure 6. Hole trap density as a function of time for different aging currents: a) scaled linearly with the aging current (≈J) and b) scaled with a ¾-power of the aging current (≈$J^{3/4}$).

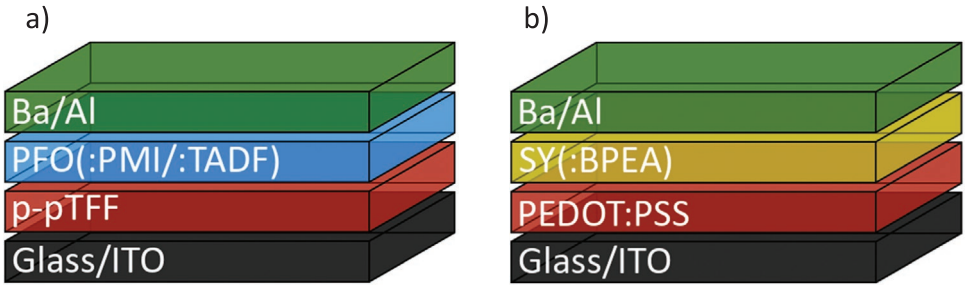

Figure 7. a) Device structure of PFO(:PMI) or PFO(:AQ(PhDPA)$_2$), where AQ(PhDPA)$_2$ is denoted as "TADF," PLEDs with p-pTFF as HIL. b) Device structure of SY(:BPEA) PLEDs with PEDOT:PSS as HIL.

To differentiate between the triplet–polaron or triplet–triplet interaction, we look at the time dependence of the hole trap density. The slope of the P_t versus *stress time* in Figure 6 (as in Figure 3c) is close to 0.5, in agreement with the earlier results on SY-PPV. As a result, also in MEH-PPV the current and stress time dependence of the hole trap formation point to triplet exciton–polaron interactions as dominant degradation mechanism. For future investigations regarding the role of singlet and triplet excitons in PLEDs we note that metalated polymers are an interesting class of materials that have been widely studied in the last decades.[54] Due to the presence of heavy metal atoms in the conjugated polymer the intersystem crossing is enhanced, such that in the emission spectrum contributions of both singlet and triplet emission can be observed. This will strongly facilitate the spectroscopic investigations of the role of triplet lifetime on PLED degradation.

4. Conclusion

In conclusion, we have experimentally disentangled the effect of singlet and triplet excitons on PLED degradation. Our results show that triplet excitons are responsible for the degradation of PLEDs, via their interactions with polarons. Lowering the singlet energy by incorporating a low concentration of fluorescent dyes does not affect PLED degradation. In contrast, addition of anthracene derivatives with long triplet lifetimes, without affecting the singlet excitons in the host, strongly enhances degradation. Furthermore, incorporation of a dye with TADF functionality with reduced triplet lifetime successfully enhances the PLED lifetime. The current and time dependence of hole trap formation under current stress provide a fingerprint for the mechanism of the degradation. The observations point to triplet exciton–polaron interactions as being the main mechanism behind the trap formation. The relatively simple PLED device structure allows for a quantitative basic understanding of the degradation, which will form a base for unravelling the degradation in more complex device architectures and more efficient ph- and TADF-based OLEDs.

5. Experimental Section

Materials: Super Yellow PPV was bought from Merck and used as received. BPEA was bought from Tokyo Chemical Industry chemicals. PFO was synthesized and purified in house. DiPP-PMI was synthesized in house. AQ(PhDPA)$_2$ was bought from Xi'an polymer light technology corp.

Device Fabrication: In a cleanroom environment prepatterned glass/indium-tin-oxide-substrates were cleaned with soap and by sonication for 10 min in both acetone and isopropanol. For SY-PPV a hole injection layer (HIL) of PEDOT:PSS (±55 nm) (Heraeus Clevios 4083) was used. For PFO a layer of high work function pTFF-C2F5SIS (±35 nm) HIL was used. PEDOT:PSS was spin coated from an aqueous dispersion and annealed at 140 °C for 10 min. P-pTFF was spin coated from acetonitrile solution after dissolving by help of an oil bath at 80 °C and mechanical shaker treatment. On top of the hole-injection layer, the active layer was spin coated in a N_2 rich environment from a chlorobenzene solution. The spin-coating parameters were set such that the thickness of the active layer ranged between 100 and 200 nm. As a last step a barium (5 nm)/aluminum (100 nm) cathode was evaporated under high vacuum conditions (±10^{-7} bar). The final device structures are given in **Figure 7**.

Device Characterization: The current–voltage (*J*–*V*) measurements were carried out with a Keithley 2400 sourcemeter in a protected environment (O_2 and H_2O values below 0.1 ppm). The photocurrent–voltage and EL measurements were carried out with a Keithley 6514 system electrometer and a USB4000 UV–vis–ES spectrometer, respectively. Thickness measurements were done with a Bruker profilometer.

Degradation Measurements: All degradation simulations were performed in a glovebox environment with oxygen and water values generally below 0.1 ppm. All measurements monitored the voltage and luminance at a constant current at room temperature.

Supporting Information

Supporting Information is available from the Wiley Online Library or from the author.

Conflict of Interest

The authors declare no conflict of interest.

Author Contributions

B.v.d.Z. and S.P. performed the experiments. R.Q.P., L.L.C. and P.K.H.H. provide p-pTFF-C2F5SIS and insight to HILs. B.v.d.Z. performed the simulations and wrote the paper with the help from co-authors. G.-J.A.H.W. and P.W.M.B. supervised the project.

Keywords

degradation, polymer light-emitting diodes, triplet–polaron interaction

Received: April 8, 2020
Revised: May 25, 2020
Published online: July 14, 2020

[1] R. H. Friend, R. W. Gymer, A. B. Holmes, J. H. Burroughes, R. N. Marks, C. Taliani, D. D. C. Bradley, D. A. Dos Santos, J. L. Brédas, M. Lögdlund, W. R. Salaneck, *Nature* **1999**, *397*, 121.
[2] J. H. Burroughes, D. D. C. Bradley, A. R. Brown, R. N. Marks, K. Mackay, R. H. Friend, P. L. Burns, A. B. Holmes, *Nature* **1990**, *347*, 539.
[3] A. J. Heeger, *Solid State Commun.* **1998**, *107*, 673.
[4] G. C. M. Silvestre, M. T. Johnson, A. Giraldo, J. M. Shannon, *Appl. Phys. Lett.* **2001**, *78*, 1619.
[5] S. Schmidbauer, A. Hohenleutner, B. König, *Adv. Mater.* **2013**, *25*, 2114.
[6] S. Scholz, D. Kondakov, B. Lüssem, K. Leo, *Chem. Rev.* **2015**, *115*, 8449.
[7] A. Gassmann, S. V. Yampolskii, A. Klein, K. Albe, N. Vilbrandt, O. Pekkola, Y. A. Genenko, M. Rehahn, H. von Seggern, *Mater. Sci. Eng., B* **2015**, *192*, 26.
[8] O. Pekkola, A. Gassmann, F. Etzold, F. Laquai, H. von Seggern, *Phys. Status Solidi A* **2014**, *211*, 2035.
[9] Y. W. Soon, H. Cho, J. Low, H. Bronstein, I. McCulloch, J. R. Durrant, *Chem. Commun.* **2013**, *49*, 1291.
[10] B. H. Cumpston, K. F. Jensen, *Synth. Met.* **1995**, *73*, 195.
[11] R. D. Scurlock, B. Wang, P. R. Ogilby, J. R. Sheats, R. L. Clough, *J. Am. Chem. Soc.* **1995**, *117*, 10194.
[12] F. So, D. Kondakov, *Adv. Mater.* **2010**, *22*, 3762.
[13] Y. Zhang, J. Lee, S. R. Forrest, *Nat. Commun.* **2014**, *5*, 5008.
[14] D.-G. Ha, J. Tiepelt, M. A. Fusella, M. S. Weaver, J. J. Brown, M. Einzinger, M. C. Sherrott, T. Van Voorhis, N. J. Thompson, M. A. Baldo, *Adv. Opt. Mater.* **2019**, *7*, 1901048.
[15] N. C. Giebink, B. W. D'Andrade, M. S. Weaver, P. B. Mackenzie, J. J. Brown, M. E. Thompson, S. R. Forrest, *J. Appl. Phys.* **2008**, *103*, 044509.
[16] S. R. Forrest, *Philos. Trans. R. Soc., A* **2015**, *373*, 20140320.
[17] J. Lee, C. Jeong, T. Batagoda, C. Coburn, M. E. Thompson, S. R. Forrest., *Nat. Commun.* **2017**, *8*, 15566.
[18] T. Furukawa, H. Nakanotani, M. Inoue, C. Adachi, *Sci. Rep.* **2015**, *5*, 8429.
[19] M. Kuik, G. A. H. Wetzelaer, H. T. Nicolai, N. I. Crăciun, D. M. De Leeuw, P. W. M. Blom, *Adv. Mater.* **2014**, *26*, 512.
[20] L. J. A. Koster, E. C. P. Smits, V. D. Mihailetchi, P, W. M. B , *Phys. Rev. B* **2005**, *72*, 085205.
[21] Q. Niu, G. A. H. Wetzelaer, P. W. M. Blom, N. I. Crăciun, *Adv. Electron. Mater.* **2016**, *2*, 1600103.
[22] Q. Niu, R. Rohloff, G. A. H. Wetzelaer, P. W. M. Blom, N. I. Crăciun, *Nat. Mater.* **2018**, *17*, 557.
[23] N. B. Kotadiya, P. W. M. Blom, G. A. H. Wetzelaer, *Nat. Photonics* **2019**, *13*, 765.
[24] M. Ariu, M. Sims, M. D. Rahn, J. Hill, A. M. Fox, D. G. Lidzey, M. Oda, J. Cabanillas-Gonzalez, D. D. C. Bradley, *Phys. Rev. B* **2003**, *67*, 195333.
[25] X. Zhang, Q. Hu, J. Lin, Z. Lei, X. Guo, L. Xie, W. Lai, W. Huang, *Appl. Phys. Lett.* **2013**, *103*, 153301.
[26] A. Perevedentsev, S. Aksel, K. Feldman, P. Smith, P. N. Stavrinou, D. D. C. Bradley, *J. Polym. Sci., Part B: Polym. Phys.* **2015**, *53*, 22.
[27] D. Neher, *Macromol. Rapid Commun.* **2001**, *22*, 1365.
[28] T. Virgili, G. Cerullo, L. Lüer, G. Lanzani, C. Gadermaier, D. D. C. Bradley, *Phys. Rev. Lett.* **2003**, *90*, 247402.
[29] T. Weil, T. Vosch, J. Hofkens, K. Peneva, K. Müllen, *Angew. Chem., Int. Ed.* **2010**, *49*, 9068.
[30] C. Ego, D. Marsitzky, S. Becker, J. Zhang, A. C. Grimsdale, K. Müllen, J. D. MacKenzie, C. Silva, R. H. Friend, *J. Am. Chem. Soc.* **2003**, *125*, 437.
[31] A. L. T. Khan, P. Sreearunothai, L. M. Herz, M. J. Banach, A. Köhler, *Phys. Rev. B* **2004**, *69*, 085201.
[32] M. A. Baldo, D. F. O'Brien, Y. You, A. Shoustikov, S. Sibley, M. E. Thompson, S. R. Forrest, *Nature* **1998**, *395*, 151.
[33] H. Spreitzer, H. Becker, E. Kluge, W. Kreuder, H. Schenk, R. Demandt, H. Schoo, *Adv. Mater.* **1998**, *10*, 1340.
[34] M. Mitsui, Y. Kawano, R. Takahashi, H. Fukui, *RSC Adv.* **2012**, *2*, 9921.
[35] V. Jankus, E. W. Snedden, D. W. Bright, V. L. Whittle, J. A. G. Williams, A. Monkman, *Adv. Funct. Mater.* **2013**, *23*, 384.
[36] Y. J. Bae, G. Kang, C. D. Malliakas, J. N. Nelson, J. Zhou, R. M. Young, Y. L. Wu, R. P. Van Duyne, G. C. Schatz, M. R. Wasielewsk, *J. Am. Chem. Soc.* **2018**, *140*, 15140.
[37] B. Arredondo, B. Romero, A. Gutiérrez-Llorente, A. I. Martínez, A. L. Álvarez, X. Quintana, J. M. Otón, *Solid-State Electron.* **2011**, *61*, 46.
[38] B. Romero, B. Arredondo, A. L. Alvarez, R. Mallavia, A. Salinas, X.Quintana, J. M. O , *Solid-State Electron.* **2009**, *53*, 211.
[39] T. van Woudenbergh, J. Wildeman, P. W. M. Blom, J. J. A. M. Bastiaansen, B. M. W. Langeveld-Vos, *Adv. Funct. Mater.* **2004**, *14*, 677.
[40] A. G. Ricciardulli, B. van der Zee, K. Philipps, G. A. H. Wetzelaer, R.-Q. Png, P. K. H. Ho, L.-L. Chua, P. W. M. Blom, *Appl. Phys. Lett. Mater.* **2020**, *8*, 021101.
[41] M. Kuik, G. A. H. Wetzelaer, J. G. Laddé, H. T. Nicolai, J. Wildeman, J. Sweelssen, P. W. M. Blom, *Adv. Funct. Mater.* **2011**, *21*, 4502.
[42] C. Wang, Y. Liu, Z. Ji, E. Wang, R. Li, H. Jiang, Q. Tang, H. Li, W. Hu, *Chem. Mater.* **2009**, *21*, 2840.
[43] L.-S. Cui, S.-B. Ruan, F. Bencheikh, R. Nagata, L. Zhang, K. Inada, H. Nakanotani, L.-S. Liao, C. Adachi, *Nat. Commun.* **2017**, *8*, 2250.
[44] Q. Zhang, H. Kuwabara, W. J. Potscavage,Jr., S. Huang, Y. Hatae, T. Shibata, C. Adachi C, *J. Am. Chem. Soc.* **2014**, *136*, 18070.
[45] B. H. Wallikewitz, D. Kabra, S. Gélinas, R. H. Friend, *Phys. Rev. B* **2012**, *85*, 045209.
[46] I. Rörich, A.-K. Schönbein, D. K. Mangalore, A. H. Ribeiro, C. Kasparek, C. Bauer, N. I. Crăciun, P. W. M. Blom, C. Ramanan, *J. Mater. Chem. C* **2018**, *6*, 10569.
[47] A. S. Dhoot, D. S. Ginger, D. Beljonne, Z. Shuai, N. C. Greenham, *Chem. Phys. Lett.* **2002**, *360*, 195.
[48] D. Abbaszadeh, A. Kunz, N. B. Kotadiya, A. Mondal, D. Andrienko, J. J. Michels, G. A. H. Wetzelaer, P. W. M. Blom, *Chem. Mater.* **2019**, *31*, 6380.
[49] D. Y. Kondakov, *Philos. Trans. R. Soc., A* **2015**, *373*, 20140321.
[50] D. Di, L. Yang, J. M. Richter, L. Meraldi, R. M. Altamimi, A. Y. Alyamani, D. Credgington, K. P. Musselman, J. L. MacManus-Driscoll, R. H. Friend, *Adv. Mater.* **2017**, *29*, 1605987.
[51] T. Shan, Z. Gao, X. Tang, X. He, Y. Gao, J. Li, X. Sun, Y. Liu, H. Liu, B. Yang, P. Lu, Y. Ma, *Dyes Pigm.* **2017**, *142*, 189.
[52] H. Lim, H. J. Cheon, G. S. Lee, M. Kim, Y.-H. Kim, J.-J. Kim, *ACS Appl. Mater. Interfaces* **2019**, *11*, 48121.
[53] V. Gray, A. Dreos, P. Erhart, B. Albinsson, K. Moth-Poulsen, M. Abrahamsson, *Phys. Chem. Chem. Phys.* **2017**, *19*, 10931.
[54] C.-L. Ho, Z.-Q. Yu, W.-Y. Wong, *Chem. Soc. Rev.* **2016**, *45*, 5264.